

Supporting Information

Eu-doped $(Y_{0.85-x}La_{0.15})_2O_3$ sesquioxide transparent ceramics for high-spatial-resolution X-ray imaging

Guiqing Feng^{a,b}, Yiheng Wu^{a,c}, Hao Lu^{a,c}, Rui Zhang^{a,b}, Shuaihua Wang^{a,d*}, Shaofan
Wu^{a,d}

^aKey Laboratory of Optoelectronic Materials Chemistry and Physics, Fujian Institute of Research on the Structure of Matter, Chinese Academy of Sciences, Fuzhou 350002, China.

^bCollege of Chemistry and Materials Science, Fujian Normal University, Fuzhou 35011, China.

^cUniversity of the Chinese Academy of Sciences, Beijing 100049, China.

^dFujian Science & Technology Innovation Laboratory for Optoelectronic Information of China, Fuzhou, Fujian 350108, China.

*Corresponding authors:

E-mail: shwang@fjirsm.ac.cn (S.H. Wang)

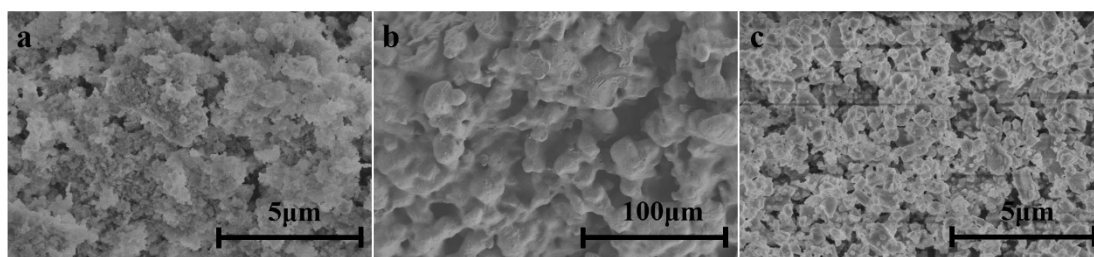


Fig. S1 a) SEM image of $(Y_{0.85}La_{0.15})_2O_3$ powder after primary ball milling. b) SEM image of $(Y_{0.85}La_{0.15})_2O_3$ powder after sintering. c) $(Y_{0.85}La_{0.15})_2O_3$ powder after secondary ball milling
Powder SEM image.

It can be seen from the powder scanning electron microscope in Fig. S1a that after one ball milling, the powder has agglomeration phenomenon, and it can be seen from Fig. S1b that the powder has agglomeration phenomenon after sintering, and the particle size becomes

larger. Fig. S1c After the second ball milling, the powder has no agglomeration and the particles are uniform.

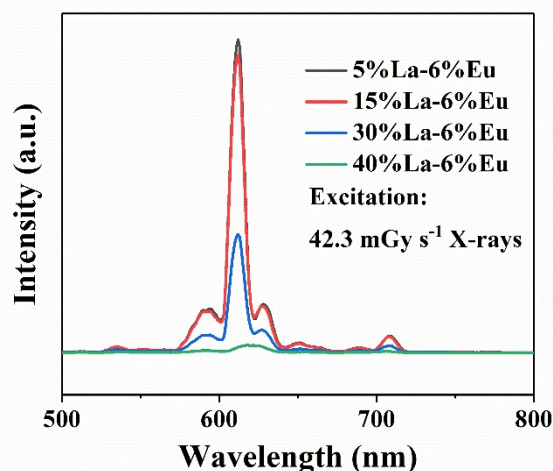


Fig. S2 RL diagram under different La³⁺ element doping

Sintering experiments were carried out with different La³⁺ ion doping when the Eu³⁺ ion doping concentration was 6% and RL tests were carried out. As can be seen from the Fig. S2, the strength values are progressively reduced with increasing La³⁺ doping. However, at 15% La³⁺ doping the strength only decreases by 5%.

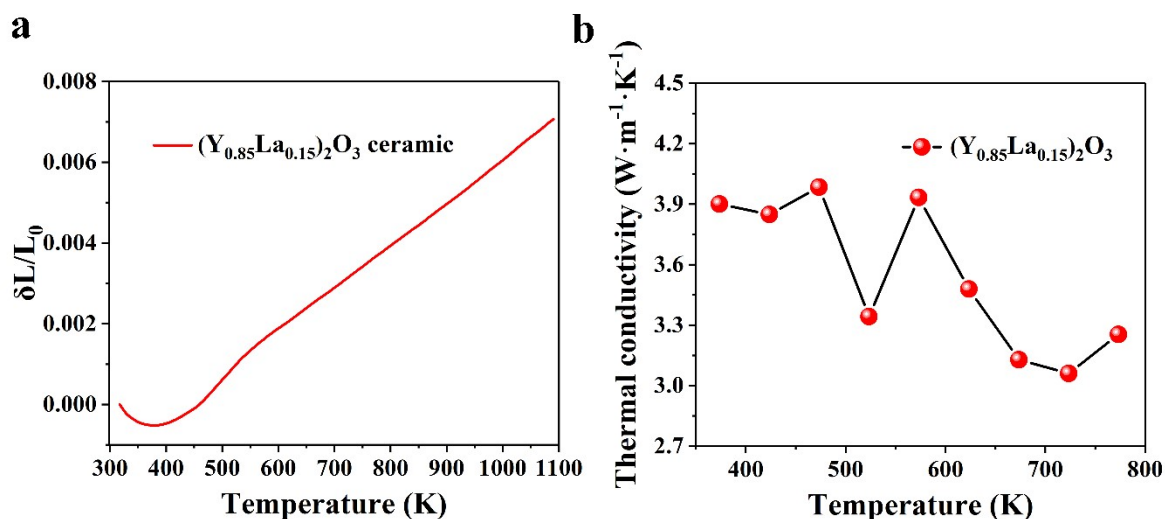


Fig. S3 a) Thermal expansion diagram of (Y_{0.85}La_{0.15})₂O₃ ceramics. b) Thermal conductivity diagram of (Y_{0.85}La_{0.15})₂O₃ ceramics.

In addition to the optical properties, thermal and mechanical performances are also important indicators for transparent ceramics. Fig. S3a is the thermal expansion diagram of (Y_{0.85}La_{0.15})₂O₃ ceramics. In the temperature range of 450 ~ 1000 K, the thermal expansion has

an approximate linear relationship with temperature, and the average thermal expansion coefficient of 450 ~ 1000 K is calculated to be $1.09 \times 10^{-5} \text{ K}^{-1}$. Fig. S3b shows the thermal conductivity of $(\text{Y}_{0.85}\text{La}_{0.15})_2\text{O}_3$ ceramic. The thermal conductivity of $(\text{Y}_{0.85}\text{La}_{0.15})_2\text{O}_3$ ceramic is calculated to be $3.90 \text{ W m}^{-1} \text{ K}^{-1}$ at 373.45 K.

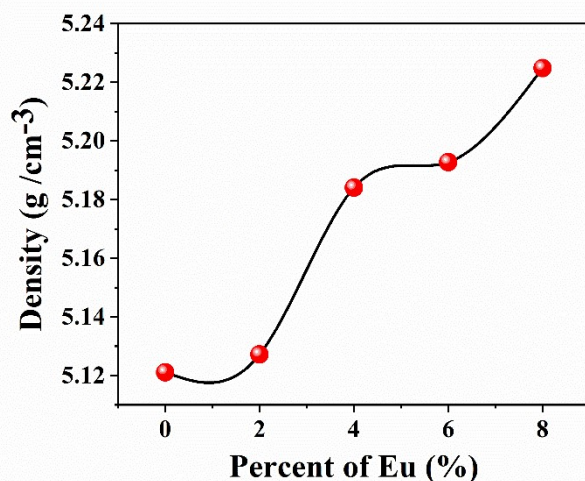


Fig. S4 Density map of different Eu doping.

Fig. S4 demonstrates that as the Eu^{3+} content increases, the density increases.

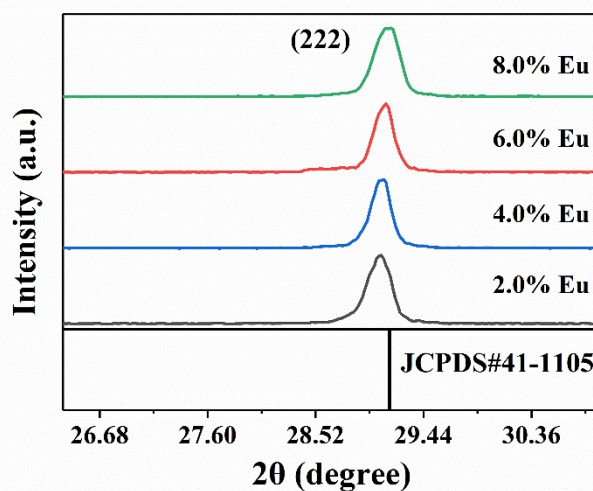


Fig. S5 XRD partial enlargement

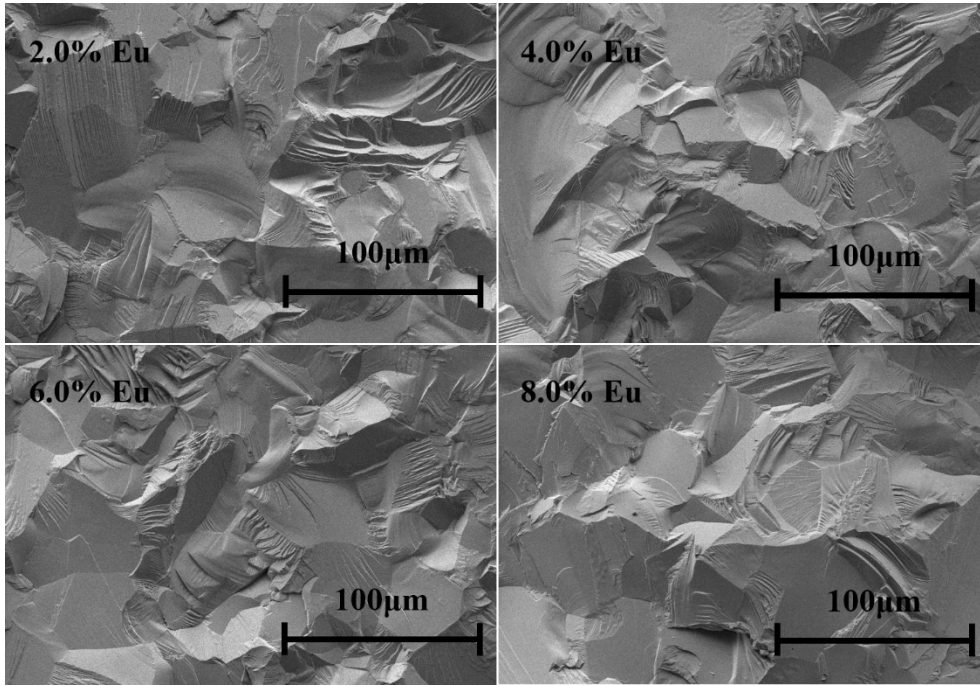


Fig. S6 Cross-sectional SEM images of $(Y_{0.85-x}La_{0.15})_2O_3:xEu$ ceramics.

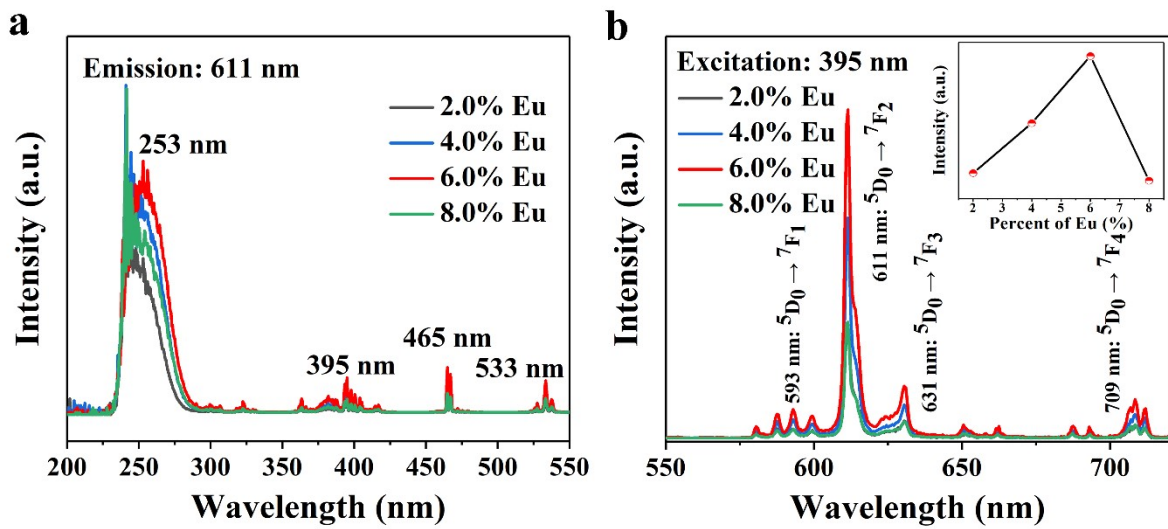


Fig. S7 a) PLE spectrum of $(Y_{0.85-x}La_{0.15})_2O_3:xEu$. b) PL spectrum of $(Y_{0.85-x}La_{0.15})_2O_3:xEu$.

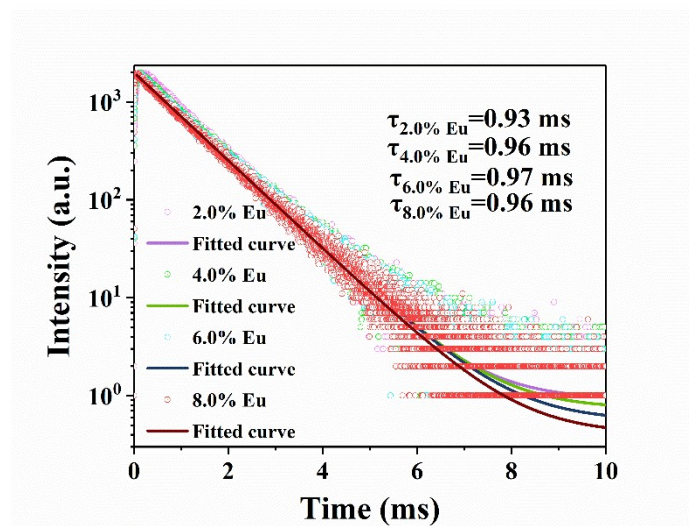


Fig. S8 Emission attenuation spectrum of $(Y_{0.85-x}La_{0.15})_2O_3:xEu$ transparent ceramic.

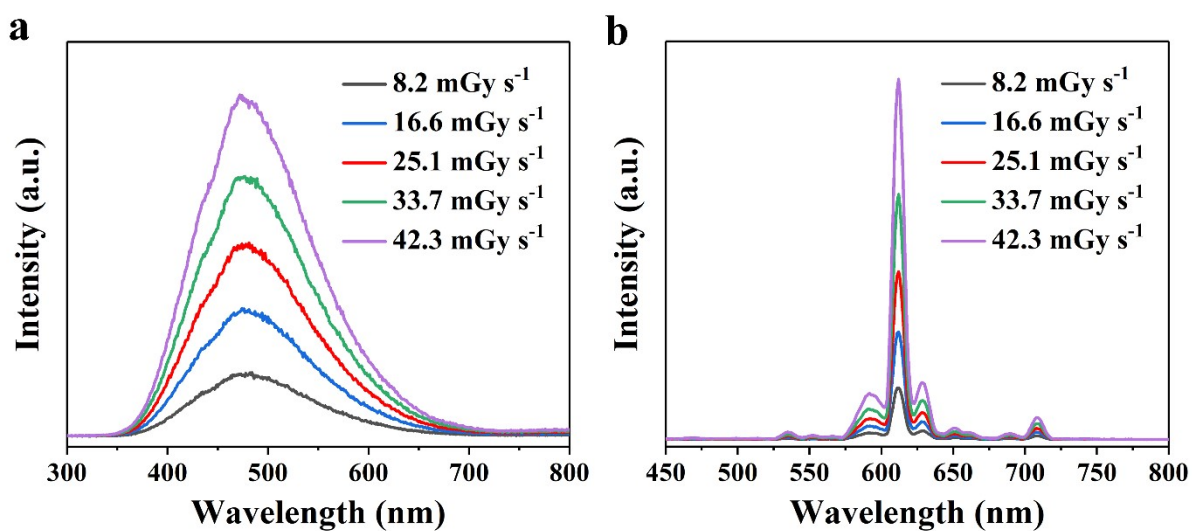


Fig. S9 a) RL maps of BGO under different doses of X-ray irradiation. b) RL maps of $(Y_{0.79}La_{0.15})_2O_3:6.0\% Eu$ under different doses of X-ray irradiation.

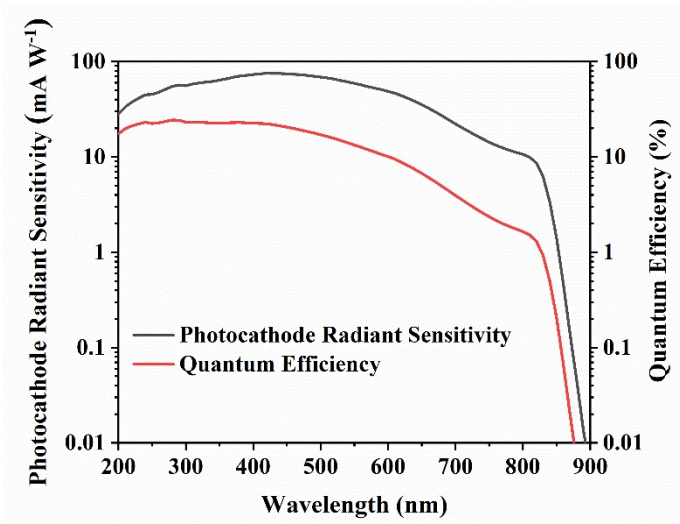


Fig. S10 The detection efficiency curve of PMT detector.

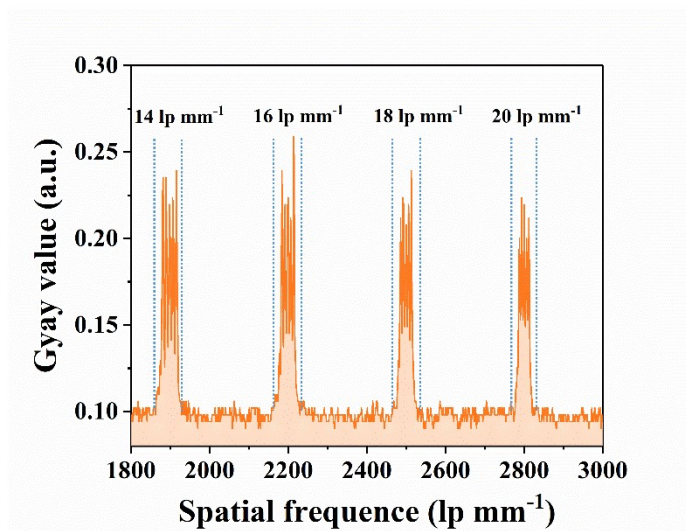


Fig. S11 Light and dark grayscale map of ceramic imaging of (Y_{0.79}La_{0.15})₂O₃: 6.0%Eu

The grayscale readings of each line pair corresponding to the light and dark stripes in the imaging map are extracted to obtain the light and dark grayscale map, as shown in Fig. S11.

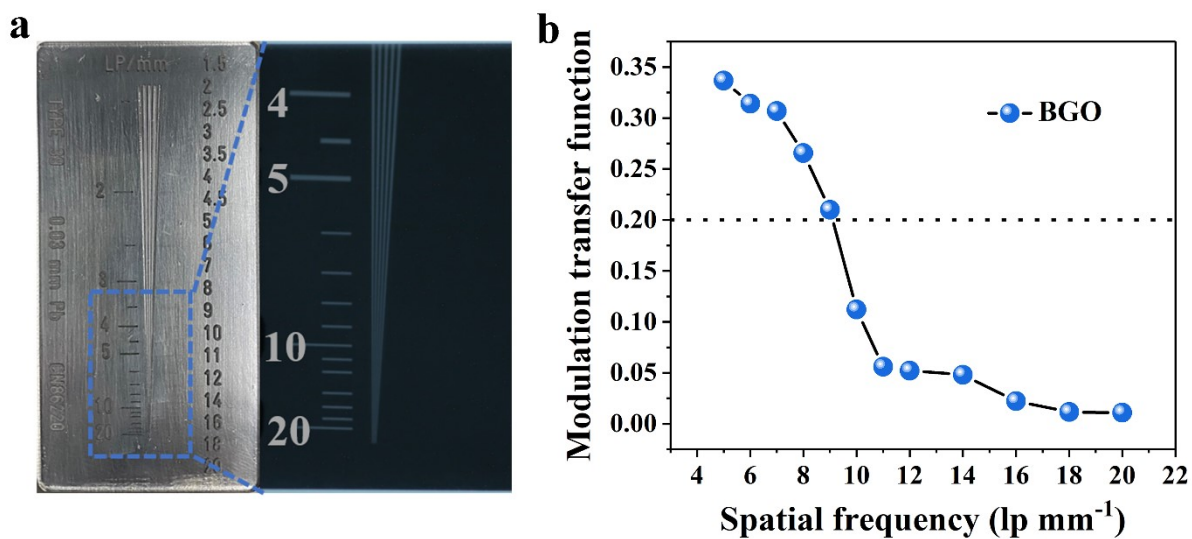


Fig. S12 a) BGO crystal imaging. b) BGO crystal MTF calculation.

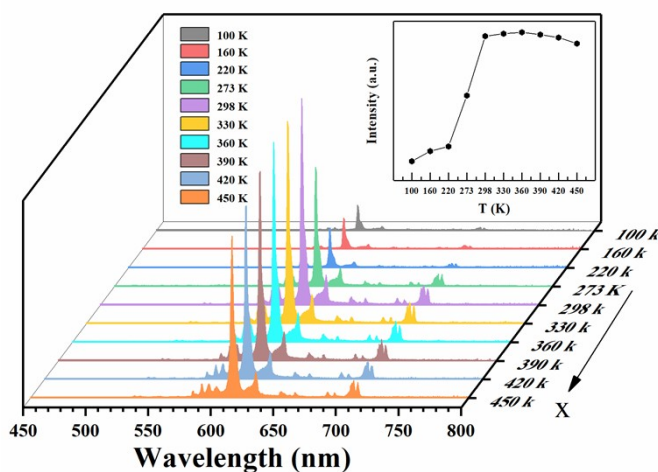


Fig. S13 Fluorescence characteristics of (Y_{0.79}La_{0.15})₂O₃: 6.0%Eu with temperature under 395 nm light excitation

The luminescence characteristics of the (Y_{0.79}La_{0.15})₂O₃:6.0% Eu sample with temperature are shown in the figure. The fluorescence luminescence intensity was measured from 100 K to 450 K under the excitation of 395 nm light. The inset of the figure also plots the sample temperature as a function. In general, an increase in temperature amplifies the population of higher vibrational levels, the density of phonons and the probability of phonon density and non-radiative transfer (energy migration to defects), and thus the emission intensity will gradually decrease. However, in Fig. S13, the luminous intensity gradually increases at

temperatures below 360 K, and gradually decreases when the temperature is higher than 360 K. Here an anomalous thermal increase behavior appears, which can be explained by the fact that thermally active phonons assist in excitation from lower to higher energy sublevels as the temperature increases.^{1,2}

References

1. S. Xin and G. Zhu, *RSC Adv.*, 2016, **6**, 41755–41760.
2. S. Liu, B. Yang, J. Chen, D. Wei, D. Zheng, Q. Kong, W. Deng and K. Han, *Angew. Chem., Int. Ed.*, 2020, **59**, 21925–21929.